arXiv:1511.08673v1 [cond-mat.str-el] 27 Nov 2015

Orbital Ordering in $Fe_{1-x}Mn_xV_2O_4$: A First Principles Study

Dibyendu Dey,[1,*] T. Maitra,[2] and A. Taraphder[1,3]

[1] *Department of Physics, Indian Institute of Technology Kharagpur, Kharagpur - 721302, India*
[2] *Department of Physics, Indian Institute of Technology Roorkee, Roorkee - 247667, India*
[3] *Centre for Theoretical Studies, Indian Institute of Technology Kharagpur, Kharagpur - 721302, India*

(Dated: November 30, 2015)

Long range orbital order has been investigated in $Fe_{1-x}Mn_xV_2O_4$ as a function of doping (x) using first principles density functional theory calculations including the effects of Coulomb correlation and spin-orbit interaction within GGA+U and GGA+U+SO approximations. Through a detailed analysis of corresponding Wannier orbital projections of the Vanadium d bands, we have clearly established that for x≤0.6, the orbital order at V sites consists of a linear superposition of d_{xz} and d_{yz} orbitals of the type $d_{xz}\pm d_{yz}$. Within each ab-plane a ferro-orbital ordering of either $d_{xz}+d_{yz}$ or d_{xz}-d_{yz} is observed which alternates in successive ab-planes along the c-direction. On the contrary, for x>0.6, it is the d_{xz} or d_{yz} orbital which orders at V sites in successive ab-planes along c-direction (so called A-type ordering). At Fe sites, we observe an orbital ordering of $d_{x^2-y^2}$ orbitals for x≤0.6 and d_{z^2} orbitals for x>0.6. Effect of spin-orbit interaction on orbital ordering is found to be not significant in the entire range of doping studied.

PACS numbers: 71.20.-b, 71.15.Mb, 71.27.+a, 71.70.Ej

I. INTRODUCTION

Correlated and frustrated electronic (spin) systems have recently observed a major surge in research activities due to the inherently rich fundamental physics involved in their understanding as well as their potential for practical applications. Vanadium spinel oxides belong to one such family of systems which, of late, has become the centre of attraction for studying phenomena involving the competition among various degrees of freedom, like spin, orbital and lattice in presence of both Coulomb correlation and geometric frustration[1,2]. These compounds with chemical formula AV_2O_4 can be broadly divided into three categories on the basis of A-site cation properties, namely; (i) A site non-magnetic (i.e. A= Zn, Mg, Cd), (ii) A-site magnetic but orbitally inactive (i.e. A = Mn, Co), (iii) A-site magnetic and orbitally active (i.e. A = Fe). As V ion is both magnetic and orbitally active, the additional magnetic and orbital degrees of freedom of A site ion bring in a very complex and rich physics with competing spin, lattice and orbital interactions (in some cases also spin-orbit interactions) in these systems. The competition among different degrees of freedom then manifests itself in several structural (accompanied often by orbital ordering) and magnetic transitions as observed experimentally in these systems.

FeV_2O_4 is a rare example among the Vanadium spinel oxides where both Fe and V cations are magnetic as well as orbitally active. This system is reported to show three successive structural transitions (cubic→ tetragonal→ orthorhombic → tetragonal) and two magnetic transitions (paramagnetic (PM) → collinear ferrimagnetic (FIM) → non-collinear ferrimagnetic (NC-FIM)) as the temperature is lowered[3–6]. Another example is MnV_2O_4 which has A-site magnetic but not orbitally active. This compound shows one structural (cubic→ tetragonal) and two magnetic (PM → FIM → NC-FIM) transitions[3,7–10]. ZnV_2O_4 can be the third example with a nonmagnetic and non-orbitally active A-site ion which undergoes one structural (cubic→ tetragonal) and one magnetic (PM → antiferromagnetic) transition[11]. Although most of the structural and magnetic transitions (along with the magnetic orders) have been unambiguously established by various experiments, the orbital order which often accompanies the structural transitions are still a matter of intense investigation and continuous debate[3,12–16].

The debate is mostly centered around the orbital order of the V sites in these spinels. V ion in its 3+ valence state has two *d*-electrons in the orbitally degenerate t_{2g} levels. In most of these systems, low temperature structure is tetragonal and VO_6 octahedra have tetragonal compression accompanied often by a trigonal distortion. Due to the tetragonal compression along z-direction the energy of the d_{xy} orbital is lowered and it is occupied by one d electron. However, the second d electron has a choice: occupy either d_{xz} or d_{yz} orbital or a combination of these two. There are various possible scenarios proposed for the orbital order in these systems based on the symmetry of the tetragonal phase and the type of dominant interactions. Some of the proposed orbital ordering models include ferro-orbital ordering of complex orbitals such as $d_{xz}\pm id_{yz}$ with dominant spin-orbit interaction[12,14], A-type antiferro-orbital ordering of real orbitals d_{xz} and d_{yz} alternating along c-direction where SO interaction is not considered strong[8,9,13] and an orbital ordering of real and complex orbitals for systems with intermediate strength of SO interaction[17,18] etc. Also, experiments have not yet been able to establish the orbital order unambiguously in these systems as there are measurements reported in the literature supporting each of these models.

Very recently, the doped variants of FeV_2O_4 and MnV_2O_4 (i.e. $Fe_{1-x}Mn_xV_2O_4$ $(0 \leq x \leq 1)$) have been studied experimentally by Kawaguchi et al.[19] and D.

Choudhuri et al.[20] where a detail magnetic and structural phase diagram has been obtained. Kawaguchi et al. have also analyzed the orbital ordering at Fe and V sites in $Fe_{1-x}Mn_xV_2O_4$ for different doping (x) on the basis of local Jahn-Teller distortions of FeO_4 tetrahedra and VO_6 octahedra respectively. From their analysis, the authors have predicted that in the range $0 \leq x \leq 0.6$, the $d_{x^2-y^2}$ orbital should order at all Fe sites and at V sites a long range ferro-orbital ordering of complex orbitals of the type $d_{xz} \pm i d_{yz}$ should be present. On the other hand, for the range $0.6 < x \leq 1$, it is the d_{z^2} orbital that orders at Fe sites and an A-type antiferro-orbital order should exist at V sites where within each ab-plane it is ferro-orbital order of either d_{xz} or d_{yz} but along c-direction it is antiferro (i.e. alternate arrangement of d_{xz} and d_{yz} orbital). However, a very recent XMCD measurements reveal that though there is a difference in the occupied orbital state in FeV_2O_4 and MnV_2O_4, the orbitals that order (at V sites) in FeV_2O_4 as well as in MnV_2O_4 are not complex but real orbitals[21]. Even though the observation of orbital order consisting of real orbitals rather than complex ones corroborates the previous theoretical predictions reported in the literature on these two systems[15,16], the exact nature of orbital ordering proposed from theory and experiments differ significantly. In view of these disagreements regarding the orbital state of parent compounds and also to study the effect of doping, we have decided to investigate the issue of orbital order in the whole range of x in $Fe_{1-x}Mn_xV_2O_4$ from a theoretical perspective using ab-initio density functional theory calculations.

II. METHODOLOGY

We have performed ab-initio density functional theory calculations within various approximations such as GGA, GGA+U and GGA+U+SO for $Fe_{1-x}Mn_xV_2O_4$ with x=0, 0.25, 0.5, 0.75 and 1. The experimental structures of parent and doped compounds have been taken from experiments[3,19,20]. In case of x=0.25 and x=0.75 we have taken the available experimental structural data for x=0.2 and x=0.8 and optimized the structure as described below. The optimization (volume, c/a ratio and oxygen positions) has been done by using Perdew-Burke-Ernzerof Generalized Gradient Approximation (PBE-GGA) exchange-correlation functional[22], within the full potential linearized augmented plane-wave (FP-LAPW) method as implemented in the WIEN2k code[23]. We have used the package 2DRoptimize available within WIEN2k package for the optimization of volume and c/a ratio. For this purpose we have considered nine different volumes around the experimental volume and for each volume nine c/a ratios were considered. During the optimization involving these 81 structures, the free internal parameters (here oxygen positions) were also optimized. Final optimized structural parameters were obtained by the analysis of the following data; (i) Energy vs. c/a for each volume, (ii) energy vs. volume (with optimized c/a) and (iii) c/a vs. volume. Each curve was then fit to 3rd, 4th and 5th order of polynomial and the lattice constants a and c were calculated from the best fit. We have listed some optimized structural parameters for x = 0, 0.5 and 0.75 in Table I which we have used for our calculations reported here. We have considered the muffin-tin radii of 2.00, 1.95, 1.65 a.u for Fe(Mn), V and O respectively. The plane wave cutoff RK_{max} was set to 8.0 for all calculations and the number of $\vec{k}$ points in the irreducible wedge of the Brillouin zone (BZ) were taken to be 60 for x = 0, 0.25, 0.5 and 72 for x = 0.75, 1. The expansion of the radial wavefunction in spherical harmonics was considered up to angular momentum quantum number $l = 10$. We also performed calculations including the correlation effects arising from the d electrons of Fe/Mn and V. For this, we have used a self-interaction corrected (SIC) GGA+U[24] approximation which takes into account the on-site Coulomb interaction U and removes the self-Coulomb and self exchange correlation energy. Spin-orbit (SO) coupling is included by the second variational method[25] with scalar relativistic wavefunctions. All the calculations were performed for the collinear ferrimagnetic spin arrangement of Fe/Mn and V ions. WANNIER90[26] and WIEN2WANNIER[27] (the interface program between WIEN2k and WANNIER90) were used to fit the bands around Fermi level by localized Wannier orbitals and to analyze the band characters in terms of these orbitals.

III. RESULTS AND DISCUSSION

On the basis of symmetry of the crystal structure and observed orbital ordering in our calculations, we divide these compounds into two groups (i) x=0, 0.25, 0.5 which we refer to as x≤0.6 case as crystal symmetry remains same in the range 0≤x≤0.6, (ii) x=0.75, 1 which we refer to as x> 0.6 case where symmetry is different from the former one.

A. $Fe_{1-x}Mn_xV_2O_4$; x=0, 0.25, 0.5

In the low temperature tetragonal phase, the crystal structures of $Fe_{1-x}Mn_xV_2O_4$ at x=0, 0.25, 0.5 have the $I4_1/amd$ symmetry as observed experimentally[3,19,20]. Our optimized structures also have the same symmetry although the local trigonal and tetragonal distortions as well as the c/a ratios differ slightly. In Table I we compared the structural parameters of experiment and optimized one for x=0.5 case. We clearly observe from Table I that the local trigonal and tetragonal distortions at FeO_4 tetrahedron and VO_6 octahedron as well as the c/a ratio of the optimized structure are comparable and more importantly have the same signs (i.e. compression or elongation along a particular direction) as the experimental one. Therefore, we discuss below the results ob-

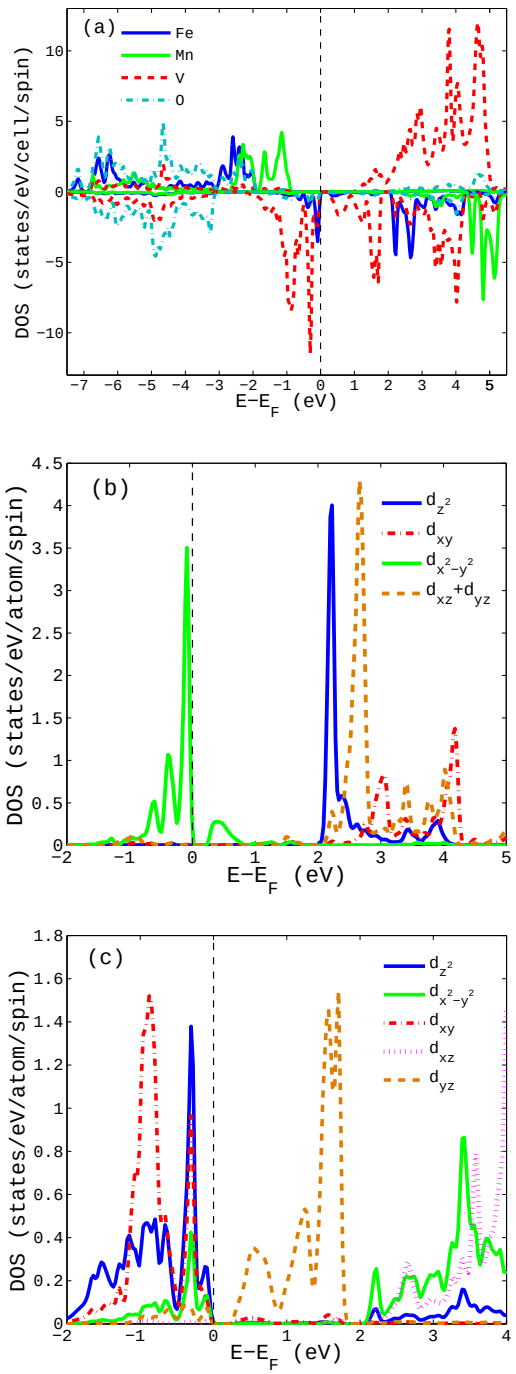


FIG. 1. (Colour online) Spin polarized DOS are shown for x=0.5. (a) Total DOS, (b) partial DOS of Fe in minority spin channel (c) partial DOS of V in majority spin channel.

tained with these optimized structures. We note that we have also performed calculations with the corresponding experimental structures where it is available and checked that our both experimental and optimized structures give consistent results.

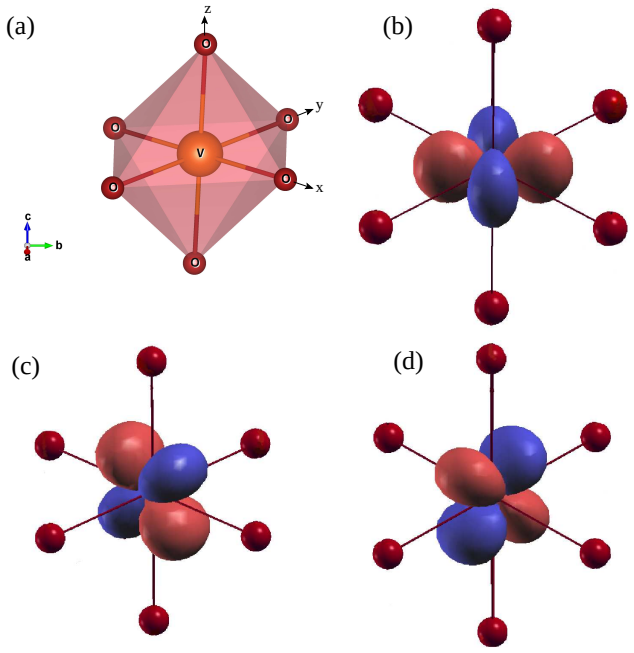


FIG. 2. (Colour online) Orientation VO_6 octahedron is shown in (a) with respect to reference frame of the tetragonal unit cell (abc) and also shown is the xyz frame in which Wannier orbitals are defined. The d_{xy}, d_{xz} and d_{yz} Wannier orbitals are shown in (b), (c) and (d) respectively.

	Lattice Constants	O-Fe-O	V-O	O-V-O
Optimized; x=0	a=5.9530, c=8.4485, c/a=1.004	107.078° (along-c) 110.681°	1.9933 A° (along-c) 2.0351 A°	85.597° 94.403°
Experimental; x=0.5	a=5.9863, c=8.4994, c/a=1.004	108.004° (along-c) 110.210°	2.0079A° (along-c) 2.0283A°	84.493° 95.507°
Optimized; x=0.5	a=5.9497, c=8.4497, c/a=1.004	108.649° (along-c) 109.884°	2.0318A° (along-c) 2.0361A°	85.612° 94.388°
Optimized; x=0.75	a=6.0502, c=8.40, c/a=0.982	111.984° (along-c) 109.884°	2.03A° (along-c) 2.032A° 2.035A°	83.715° 96.285°

TABLE I. Structural parameters and various distortions observed in the optimized structures for x=0, x=0.5 and x=0.75 are listed. Corresponding experimental data is also given in case of x=0.5 case for comparison[20].

GGA+U Results: As both parent compounds (FeV_2O_4 and MnV_2O_4) as well as the doped ones are known to be Mott insulators, we have included in our calculations the Coulomb correlation within GGA+U approximation. The calculations have been performed for various values of U_{eff} ($= U - J$, where U is on-site Coulomb interaction and J is the Hund's exchange interaction strength) ranging from 3eV to 5eV at Fe, Mn

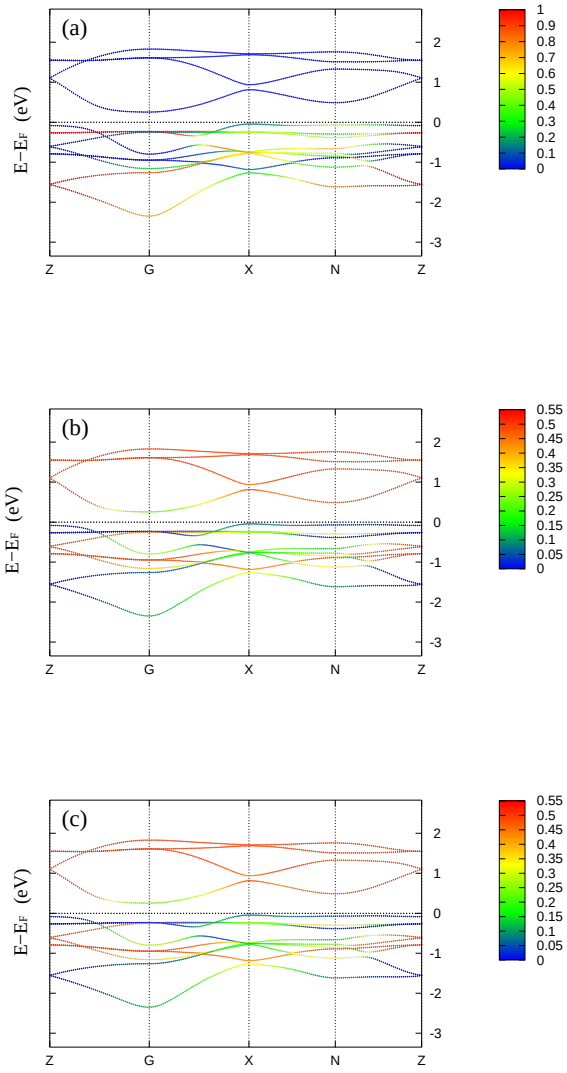


FIG. 3. (Colour online) Projections of V t_{2g} bands on to d_{xy}, d_{xz} and d_{yz} Wannier orbitals are shown for x=0.5 in (a), (b) and (c) respectively. It is seen that d_{xy} has the lowest energy and it is fully occupied while d_{xz} and d_{yz} are occupied with equal weight.

and V sites. We note that conclusions drawn from our calculations do not change when we vary the values of U_{eff} in the above range. Therefore, we present below the results obtained for the U_{eff} value of 4eV (3eV) at Fe/Mn (V) sites. In addition, in all our calculations we have considered collinear ferrimagnetic order among the Fe (Mn) and V spins (i.e. V spin moments are aligned opposite to Fe (Mn) spin moments).

Our primary goal here is to ascertain the type of ground state orbital order in these systems. As mentioned above we observed qualitatively similar behaviour as far as the orbital order is concerned for x=0, 0.25 and 0.5. Therefore, we present the case of x = 0.5 in detail below. In Fig. 1(a) we show the total density of states (DOS) of Fe, Mn, V and O in both the spin channels within GGA+U approximation. Consistent with the experimental observation the insulating ground state with a gap of about 0.2eV is obtained. Furthermore, we see that due to the tetrahedral crystal field, the Fe d- states are split into t_{2g} and e_g with e_g states having lower energy. The valence state of Fe is 2+ as the spin up (majority) states are fully filled by 5 d electrons and spin down (minority) e_g states are partially filled by one electron. Partial filling of the minority e_g states causes Jahn-Teller effect which in turn further splits these states to lower energy $d_{x^2-y^2}$ and higher energy d_{z^2} state. This energy level splitting can be understood by looking at the local distortions of FeO_4 tetrahedron presented in Table I. In the high temperature cubic phase, all six interior O-Fe-O bond angles are degenerate having a value 109.4^o. Whereas, in the low temperature tetragonal phase FeO_4 tetrahedron is elongated along c-direction making $d_{x^2-y^2}$ the ground state orbital. Therefore, the minority spin electron occupies $d_{x^2-y^2}$ orbital as we can see in the partial DOS of Fe d-states in the minority spin channel presented in Fig 1(b).

Similarly, Vanadium d-states are split into t_{2g} and e_g with t_{2g} states having the lower energy due to octahedral crystal field. Majority (here spin down due to ferrimagnetic ordering) t_{2g} states are partially filled by two d electrons. Unlike FeO_4 tetrahedron (where all Fe-O bond lengths are equal), VO_6 octahedron has both tetragonal and trigonal distortions in the low temperature tetragonal phase (see Table I). There is a compression of V-O bonds along c-direction compared to four equal V-O bonds in the ab-plane. In addition, there also exists a trigonal distortion (i.e. O-V-O bond angles deviating from 90^o) in the ab-plane as well as out of ab-plane. Because of the presence of tetragonal compression along c(z) direction the degeneracy of the t_{2g} states is further lifted and d_{xy} band moves to a lower energy below Fermi level (FL) and gets fully occupied by one electron. One can clearly observe this from the partial DOS of V d-states (in majority spin channel) presented in Fig 1(c). We also observe from Fig 1(c) that there is a further splitting of the remaining two t_{2g} states to accommodate the second electron giving rise to the insulating gap at the FL. The later splitting of t_{2g} states happens due to the orbital ordering. In order to find out the orbital character of the second highest occupied state , we have calculated the projections of three Wannier orbitals as shown in Fig 2 of the Vanadium d-bands around the FL. The corresponding projections are shown in Fig 3(a), (b) and (c) for d_{xy}, d_{xz} and d_{yz} orbitals respectively. From these figures we can clearly establish that d_{xy} orbital character is the most dominant one among the lower energy bands and it's peak has a lower energy than the other two. It appears only below FL and hence fully occupied which is

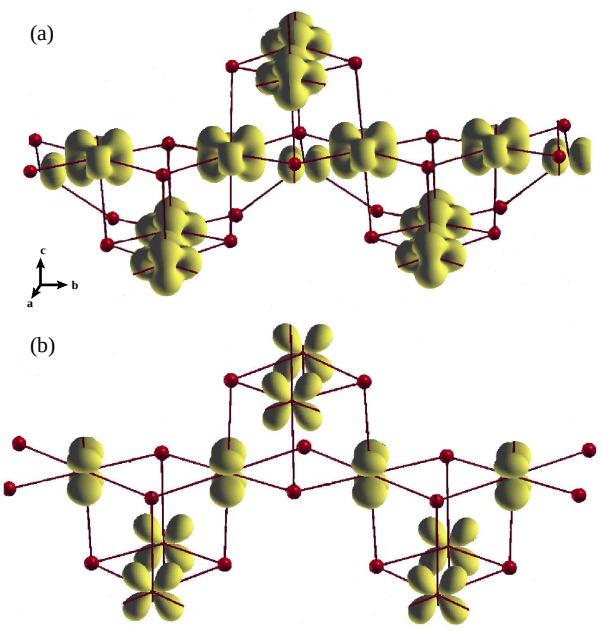


FIG. 4. (Colour online) 3D electron density is shown in real space lattice for x=0.5 case in (a). Corresponding hole densities are shown in (b) to depict the nature of unoccupied orbitals.

expected because of the compression of V-O bonds along c(z)-direction. Interestingly we further observed that the d_{xz} and d_{yz} characters of exactly equal proportions are present in higher energy bands (i.e. close to FL) and these are partially filled. This implies that d_{xy} orbital has the lowest energy and it is filled by one electron but the 2nd electron occupies equally d_{xz} and d_{yz} orbitals (i.e. a linear superposition of d_{xz} and d_{yz} orbitals).

In order to find out the type of long range orbital order that exists in these systems and the exact composition of the orbitals that order we calculated the 3D electron density in real space and presented it in Fig. 4(a) (for x=0.5). As expected we can now clearly see that there is an ordering of $d_{x^2-y^2}$ orbitals at all Fe sites. The V orbitals ordering however is more complicated. In each ab-plane V orbitals are ferro-orbitally ordered with the second electron occupying either $\frac{1}{\sqrt{2}}(d_{xz}+d_{yz})$ or $\frac{1}{\sqrt{2}}(d_{xz}-d_{yz})$ at all V sites. As we move along c-direction, in successive ab-planes we observe $\frac{1}{\sqrt{2}}(d_{xz}+d_{yz})$ or $\frac{1}{\sqrt{2}}(d_{xz}-d_{yz})$ alternately ordered. To depict this clearly we have also plotted the corresponding hole densities (i.e. for V states just above FL) of V chains in adjacent ab-planes (see Fig 4(b)). The staggered orbital order along c-direction can be clearly seen here. We observe from Fig. 4 that the electron orbitals point towards each other along a V chain whereas hole orbital point away from each other which could be understood on the basis of kinetic energy gain due to more overlap between the neighbouring V orbitals.

GGA+U+SO Results: As it is established from various experimental and theoretical studies that some of these Vanadium spinel oxides also show dominant spin-orbit (SO) interaction effect which then leads to the orbital ordering of complex orbitals rather than real ones[12,14], we have included SO interaction in our calculations through GGA+U+SO approximation. However, in the entire series of compounds studied, the effect of SO interaction was not found to be significant either on the electronic structure or on the orbital ordering. Orbital moments also observed to be quite small compared to, for example, ZnV_2O_4 where it is found to be large. We list the calculated orbital moments for Fe and V for different doping in Table II. Interesting, in a recent XMCD measurement, Nii et al. also observed negligible orbital moment in both FeV_2O_4 and MnV_2O_4[21]. Therefore, we conclude that the long range orbital order that is present at V and Fe sites as discussed above involves only real orbitals not the complex ones such as $d_{xz}\pm id_{yz}$ which was observed in case of ZnV_2O_4[12,14].

B. $Fe_{1-x}Mn_xV_2O_4$; x=0.75, 1

In experiments it has been observed that in x>0.6 regime, $Fe_{1-x}Mn_xV_2O_4$ has $I4_1/a$ symmetry in the tetragonal phase at low temperature and c/a ratio is less than 1 unlike x≤0.6 case where it has $I4_1/amd$ symmetry and c/a ratio above 1. Therefore, the local distortions at FeO_4 tetrahedra and VO_6 octahedra are very different from that observed in x<0.6 cases discussed in the previous section (refer to x=0.75 case in Table I). We observe that in these cases both FeO_4 tetrahedra as well as VO_6 octahedra are compressed along c-direction. In addition, in the VO_6 octahedra four V-O bonds of the ab-plane are split into two short and two long bonds as opposed to the cases below x=0.6 where all four V-O bonds in the ab-plane had equal magnitude. These long/short bonds alternately point along x or y-direction (refer to the Fig 2(a)) in successive ab-planes as one moves along c(z)-direction. Trigonal distortions are also present as listed in Table I.

We performed electronic structure calculations for $Fe_{1-x}Mn_xV_2O_4$ at x=0.75 and 1 within GGA+U and GGA+U+SO approximations as we discuss below. As the electronic structure and the orbital order (at V sites) are found to be similar in nature for x=0.75 and x=1 we present the results for x=0.75 case.

GGA+U Results: In Fig.5 we show the partial DOS for Fe and V d-states in minority and majority spin channels respectively within GGA+U with U_{eff}=4eV and 3eV at Fe(Mn) and V sites. By looking at the partial DOS of minority Fe d-states we see that JT distortion in this case makes d_{z^2} the ground state. This is consistent with the compression of FeO_4 tehedra along c(z)-direction. However, the Vanadium d-states undergo a complicated splitting with all t_{2g} orbital (i.e. d_{xy}, d_{xz}, d_{yz}) characters being present above and below FL. This is understandable as VO_6 octahedra undergo local and co-

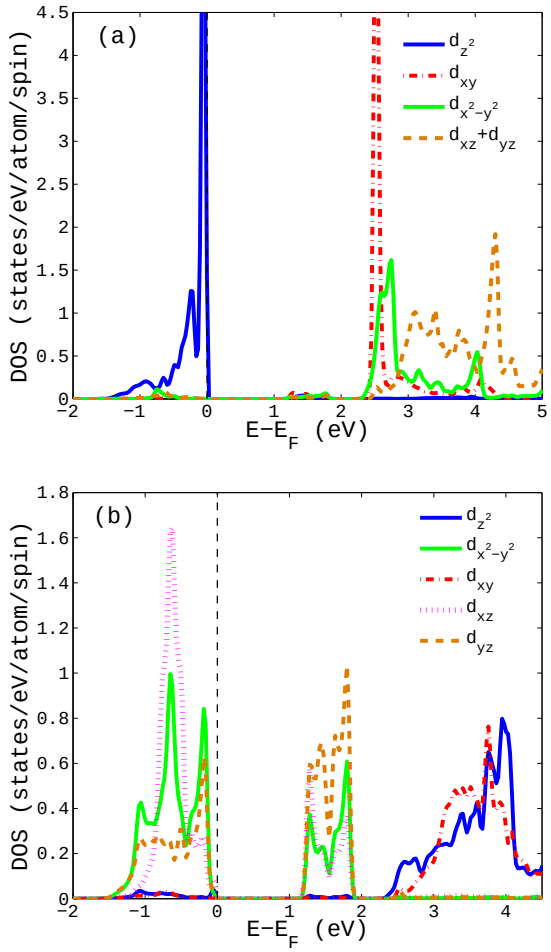


FIG. 5. Spin polarized DOS are shown for x=0.75. (a) Partial DOS of Fe in minority spin channel (b) partial DOS of V in majority spin channel.

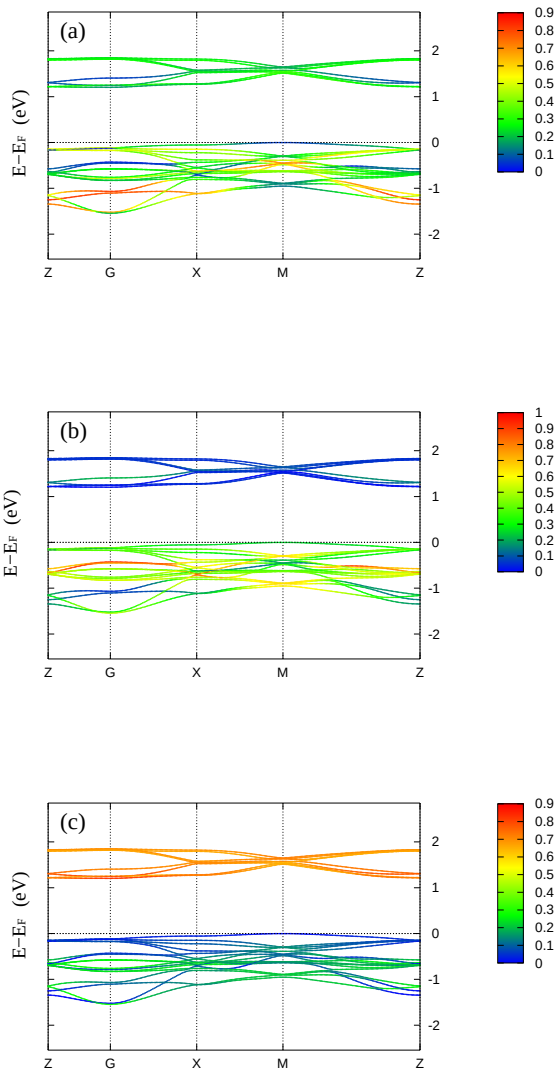


FIG. 6. (Colour online) Projections of V t_{2g} bands on to d_{xy}, d_{yz} and d_{xz} Wannier orbitals are shown for x=0.75 in (a), (b) and (c) respectively.

operative JT distortions (both tetragonal and trigonal) leading to orbital ordering. Similar to the previous cases of x≤0.6, we have analysed the orbital characters by calculating the corresponding Wannier orbital projections of the V t_{2g}-bands above and below FL. We show these projections in Fig. 6. Consistent with the JT compression along c-direction, the lowest bands have high contribution from d_{xy} orbital. However, in a significant deviation from the earlier case (i.e. x≤0.6), here we observe that d_{xz} and d_{yz} are not equally populated. The filled states below FL have dominant contribution from d_{yz} orbital (about 80% or so) whereas d_{xz}'s presence is very small (about 20% or so). This implies that the lowest occupied orbital is predominantly d_{xy} in nature whereas the next higher occupied orbital is d_{yz} in nature as also observed in case of MnV_2O_4[15]. The polarization of the second highest occupied orbital (i.e. lifting of the degeneracy of d_{xz} and d_{yz}) is consistent with the JT distortion which causes the splitting of V-O bonds in the ab-plane into two short and two long ones as mentioned above. Interestingly, we further observed by plotting the corresponding Wannier orbitals in real space that the polarization (ordering) character of the second highest occupied state alternate in successive ab-planes along c-direction. If in one ab-plane it is the d_{yz} which gets polarized (ordered), then in the next ab-plane it is the d_{xz} that becomes the second most populated orbital. This keeps repeating so that the second d-electron of V^{3+} occupies alternately d_{xz} and d_{yz} as we move along c-direction. Note that d_{xy} remains the most populated orbital at all V sites. This is often referred to as A-type orbital ordering in the literature[8,19,20]. The staggered ordering of d_{xz} and d_{yz}

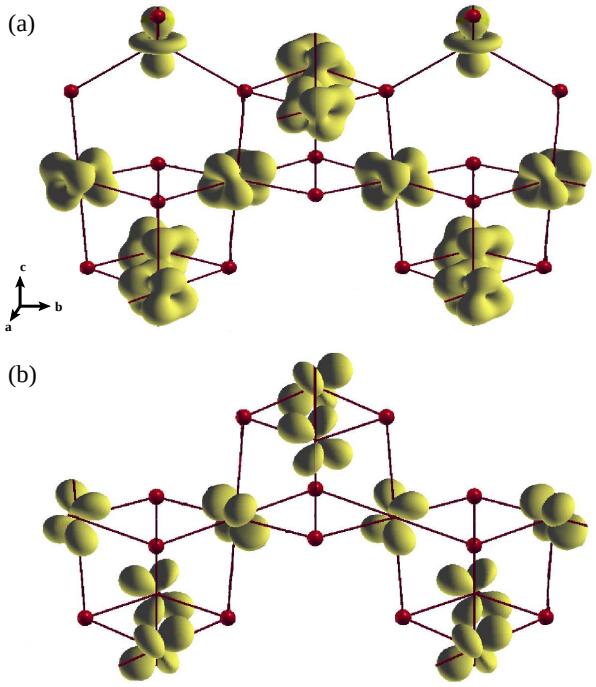


FIG. 7. 3D electron density is shown in real space lattice for x=0.75 case in (a). Corresponding hole densities are shown in (b) to depict the nature of unoccupied orbitals.

	Fe (μ_B)	V (μ_B)
x=0.5	0.11	0.22
x=0.75	0.00	0.07

TABLE II. Calculated orbital moments of Fe and V ions in doped systems.

orbital along c(z)-direction can be understood if we look at the JT distortion which is also also staggered along the same direction as described above. If two longer V-O bonds are pointed along x-direction (refer to Fig. 2(a)) then the second highest occupied orbital has dominant d_{xz} character and if two longer V-O bonds are pointed along y-direction then the second highest occupied orbital has dominant d_{yz} character.

In Fig.7 we present the 3D electron density in real space for x=0.75 of $Fe_{1-x}Mn_xV_2O_4$. We clearly see the d_z^2 orbitals at Fe sites. The electron density at V sites are similar to that obtained for the parent compound MnV_2O_4. There is a tilting of occupied orbitals within each V chain in the same ab-plane which was also seen in MnV_2O_4[15]. This tilting of orbitals along the V chains is caused by the trigonal distortion present. However, the orbital ordering remains same as we go along the V chains either in a or b direction. Therefore, the orbital ordering at V sites as discussed above is applicable to both x=0.75 and x=1. We have verified this through Wannier orbital projection analysis as presented above for x=1 as well.

GGA+U+SO Results: We also performed calculations including SO interaction to study its effect on orbital ordering and whether there are complex orbitals involved in the ordering process. However, we did not observe any significant effect of SO interaction in this case either. The calculated orbital moments are also found to be very small as listed in Table II. V orbital moment is found to be about $0.07\mu_B$ which is much smaller than that found for x=0.5 case (i.e. $0.22\mu_B$). This is consistent with the observation of Kawaguchi et al. that above x=0.6 the orbital moments should decrease. The observation of low orbital moment is also consistent with the recent XMCD measurements and previous theoretical calculations on MnV_2O_4[15,21]. Therefore, we conclude that the orbital ordering involves only real orbitals in this case as well.

IV. CONCLUSIONS

We have performed first principles density functional theory calculations in a series of compounds $Fe_{1-x}Mn_xV_2O_4$ with x = 0, 0.25, 0.5, 0.75 and 1 where experimental measurements related to orbital ordering have recently been reported. We investigated in detail the orbital ordering of Fe and V d-orbitals in these systems from our calculations under various approximations such GGA, GGA+U and GGA+U+SO. We have also performed a detail analysis of long range orbital order by calculating the Wannier orbital projections of the occupied d-bands and plotting those orbitals in real space lattice. On the basis of the observed orbital order from our calculations we divide these systems into two classes; one which includes the compounds x=0,0.25 and 0.5 and the other includes x=0.75 and 1. In the former, we observe $d_{x^2-y^2}$ orbital order at Fe sites while in the later it is d_{z^2} orbital ordering. As far as V sites are concerned, in the former case, d_{xy} orbital is found to be present at all V sites as expected and the second orbital that is ordered has equal contribution from d_{xz} and d_{yz} (i.e a linear superposition of the type d_{xz}+d_{yz} or d_{xz}-d_{yz}). In successive ab-planes along c-direction the composition of this orbital alternates between d_{xz}+d_{yz} and d_{xz}-d_{yz}. We further observe that real orbitals, not complex ones as had been claimed in some reports earlier[19], are involved in the orbital ordering process. This observation is consistent with the recent XMCD measurements on the parent compounds[21]. For x=0.75 and 1, we observe, apart from d_{xy} orbital being present at all V sites, the second electron occupies preferentially either d_{xz} or d_{yz} in successive ab-planes as one moves along c-direction which is often referred to as A-type orbital ordering in the literature.

V. ACKNOWLEDGMENTS

Authors acknowledge D. Choudhuri for useful discussions particularly on experimental observations in these

systems. DD acknowledges DST Inspire (India) for research fellowship. TM acknowledges CSIR (India) for funding under the project grant no: 03(1212)/12/EMR-II.

* dibyendu@phy.iitkgp.ernet.in

[1] S. H Lee, *et al.*, J. Phys. Soc. Jpn. **79**, 011004 (2010).
[2] P. G. Radaelli, New J. Phys. **7**, 53 (2004).
[3] Y. Nii, H. Sagayama, T. Arima, S. Aoyagi, R. Sakai, S. Maki, E. Nishibori, H. Sawa, K. Sugimoto, H. Ohsumi, and M. Takata, Phys. Rev. B **86**, 125142 (2012).
[4] T.Katsufuji, T. Suzuki, H. Takei, M. Shingu, K. Kato, K. Osaka, M. Takato, H. Sagayama, and T. Arima, J. Phys. Soc. Jpn. **77**, 053708 (2008).
[5] G. J. MacDougall, V. O. Garlea, A. A. Aczel, H. D. Zhou, and S. E. Nagler, Phys. Rev. B **86**, 060414(R) (2012).
[6] Kang J-S *et al.*, Phys. Rev. B **85**, 165136 (2012).
[7] T. Suzuki, M. Katsumura, K. Taniguchi, T. Arima, and T. Katsufuji, Phys. Rev. Lett. **9**8, 127203 (2007).
[8] V. O. Garlea, R. Jin, D. Mandrus, B. Roessli, Q. Huang, M. Miller, A. J. Schultz, and S. E. Nagler, Phys. Rev. Lett. **100**, 066404 (2008).
[9] H. Tsunetsugu and Y. Motome, Phys. Rev. B **68**, 060405(R) (2003).
[10] K. Adachi, T. Suzuki, K. Kato, K. Osaka, M. Takata, and T. Katsufuji, Phys. Rev. Lett. **95**, 197202 (2005).
[11] M. Reehuis, A. Krimmel , N. Buttgen, A. Loidl , and A. Prokofiev, Eur. Phys. J. B **35**, 311 (2003).
[12] O. Tchernyshyov, Phys. Rev. Lett. **93**, 157206 (2004).
[13] Y. Motome and H. Tsunetsugu, Phys. Rev. B **70**, 184427 (2004).
[14] T. Maitra and R. Valenti, Phys. Rev. Lett. **99**, 126401 (2007).
[15] S. Sarkar, T. Maitra, R. Valenti, and T. Saha-Dasgupta, Phys. Rev. Lett. **102**, 216405 (2009).
[16] S. Sarkar and T. Saha-Dasgupta, Phys. Rev. B **84**, 235112 (2011).
[17] E.M. Wheeler, B. Lake, A.T. M. Nazmul Islam, M. Reehuis, P. Steffens, T. Guidi and A. H. Hill, Phys. Rev. B **82**, 140406(R) (2010).
[18] R. Kaur, T. Maitra and T. Nautiyal, J. Phys.: Condens. Matter **25**, 065503 (2013).
[19] S.Kawaguchi, H.Ishibashi, J.Kim and Y.Kubota, J. Phys.: Condens. Matter **26**, 346001 (2014).
[20] D. Choudhuri *et al.*, Phys. Rev. B **89**, 104427 (2014).
[21] K. Matsuura, H. Sagayama, Y. Nii, N. D. Khanh, N. Abe, and T. Arima, Phys. Rev. B **92**, 035133 (2015).
[22] J. P. Perdew, A. Ruzsinszky, G. I. Csonka, O. A. Vydrov, G. E. Scuseria, L. A. Constantin, X. Zhou and K. Burke, Phys. Rev. Lett. **100**, 136406 (2008).
[23] P. Blaha, K. Schwartz, G. K. H. Madsen, D. Kvasnicka and J. Luitz, 2001 WIEN2k ed K Schwarz.
[24] V. I. Anisimov, I. V. Solovyev, M. A. Korotin, M. T. Czyzyk and G. A. Sawatzky, Phys. Rev. B **48**, 16929 (1993).
[25] D. D. Koelling and B. N. Harmon, J. Phys. C: Solid State Phys. **10** 3107 (1977).
[26] A. A. Mostofi, J. R. Yates, Y.-S. Lee, I. Souza, D. Vanderbilt and N. Marzari, Comput. Phys. Commun. **178**, 685 (2008).
[27] J. Kunes, R. Arita, P. Wissgott, A. Toschi, H. Ikeda, K. Held, Comp.Phys.Commun. **181**, 1888 (2010).